

## EFFECT OF MWCNT LOADINGS IN MWCNT/PEO COMPOSITES AS ACETONE SENSORS

N. B. MOHAMMED<sup>\*a</sup>, F. A. RAZAK<sup>b</sup>, R. MD NOR<sup>b</sup>, N. BENOUEATTAS<sup>c</sup>

<sup>a</sup>*Department of Sciences and Techniques, Faculty of Sciences and Technology, University of Bordj-Bou-Argeridj 34000, Algeria*

<sup>b</sup>*Department of Physics, Faculty of Science, University of Malaya, 50603 Kuala Lumpur.*

*Noureddine Benouattas*

<sup>c</sup>*Department of Physics, Faculty of Sciences, University of Ferhat Abbas, Setif 19000, Algeria.*

In this paper, we report a study on the behavior of PEO/MWCNT composites as acetone vapour sensors. PEO/MWCNT composites were fabricated at MWCNT loadings of 5 to 50% wt. using the solution casting method. Dried composite films were analyzed using Raman spectroscopy and FESEM. Acetone sensors were fabricated from dried composite films by monitoring resistance changes due to acetone vapor exposure. Sensor responses were measured as a function of airflow rates bubbled through a solution of acetone in water. Effects on sensor response and sensitivity for sensors made up of composites with different MWCNT loadings were studied. MWCNTs were found to be well dispersed in the composite based on Raman spectroscopy analysis. Acetone sensing using the PEO/MWCNT composite showed a trend where sensitivity increased with decreasing MWCNT loadings but with saturation of measurements at high acetone concentration. This phenomenon was explained in terms of the electrical conductivity mechanism in MWCNT, which involved the immobilization of carrier electrons in the MWCNT. Our results demonstrated that as the sensitivity of the sensor increased with decreasing MWCNT loadings, saturation of measurements increased with increasing MWCNT loadings.

(Received April 30, 2016; Accepted July 1, 2016)

*Keywords:* Multiwalled carbon nanotubes, Polyethylene oxide, Composites, Acetone sensors.

### 1. Introduction

Acetone is one of the flammable volatile gases, inhaling or exposing to acetone, especially to high concentrations, can irritate and harm several organs of the human body [1]. Since acetone is commonly used, its concentration in the work place should not exceed 400mg/m<sup>3</sup> for safety purpose [2]. Meanwhile, acetone is arguably the most important chemical marker detected in the exhaled breath of diabetic patients [3]. Diabetes disease makes a third of the death toll in the industrialized countries [4]. Acetone concentration ranges from 1.7 ppm to 3.7 ppm could be detected in breath of diabetics compared to healthy humans with typically less than 0.8 ppm [5]. Hyperketonaemia disease associated with cattle can be detected by monitoring the concentrations of breath acetone [6]. Hence, detection and measurement of acetone gas is of great significance in health protection and diagnosis. As such the techniques for the monitoring of acetone are of great interest. Different methods have been used to assess breath acetone, such as semiconductor gas sensor, gas chromatography [7] GC-ion mobility spectrometry (GC-IMS) [8]. Laser spectroscopic techniques based on cavity ring down spectroscopy (CRS) [9,10], in addition to MOS e-nose [11] and Differential Mobility Sensor (DMS) [12].

---

\* Corresponding author: nadjima2004@yahoo.com

Multiwalled carbon nanotubes (MWCNT) based sensors including gas sensors have received much attention due to the special properties of MWCNTs. However, the use of pure MWCNT is not practical because of adhesion problem where MWCNT are powderized when dry. To overcome the powder handling difficulties, it is mixed with polymers to form composites. One example is polyethylene oxide (PEO) which is a flexible polymer that is miscible in water. Fabrication of PEO/MWCNT composites and studies on their electrical, mechanical and rheological properties has been reported [13-15]. In all these studies, the excellent electrical properties were reported with percolation threshold of as low as 0.5-1% mass loading of MWCNT [14]. The enhanced electrical properties due to MWCNT loading can be utilized as organic vapor sensors. In the percolated network of the conducting MWCNT fillers in the polymer matrices, electrons flow through the direct contact of MWCNT or by tunneling between the adjacent tubes at close distances[16]. The main reason behind the resistance change when conducting polymer/MWCNT composites are exposed to organic vapors is the disconnection of conducting pathways, resulting from the immobilization  $\pi$ - electrons on the MWCNT surfaces due to the absorption of vapor molecules [17].

The conventional gas semi conducting metal oxide based gas sensors have provided good results. However, they have needed high temperatures for their functioning, such as 150 °C , 220°C, 425 °C regarding TiO<sub>2</sub> [18], ZnO [19]andWO<sub>3</sub>[20]respectively. High working temperature affects sensor stability and consume high thermal energy. The use of polymer-CNT composites as vapor sensors has many advantages, for example, it is cheap, portable due to small size, has room temperature operation, good reproducibility, environmental stability and fast response [17]. Hence, several studies have discussed the applicability of polymer-CNT composites for vapor sensing [21-23].

In this paper, we report the result of a study on the effect of MWCNT loading in PEO/MWCNT composite on the response to acetone vapour. Composites containing 5, 15, 25, 33, 40 and 50% wt. of MWCNTs in PEO were prepared and exposed to vapor containing acetone evaporated from a solution of acetone in water. The concentration of acetone was varied by varying the flow rate of air through a solution of 25% acetone in water.

## 2. Experimental details

MWCNT of 95% purity, >50nm diameter and lengths between 10 and 15  $\mu\text{m}$  were obtained from Chengdu Organic Chemicals Limited, China, and was used as received. The MWCNT was dispersed ultrasonically using sodium dodecyl sulphate (SDS) solution. Typically 1wt. % MWCNT in 1% wt. solution of SDS in deionized water was sonicated for 1 hour at 25 W to obtain a stable suspension. Fabrication of the PEO/MWCNT composite was by the solution casting method. Typically, samples of 1g PEO was dissolved in 50 ml DI water. Under continuous stirring MWCNT suspension containing different mass of MWCNT was added to the PEO/MWCNT solution. After being thoroughly mixed, it was then subjected to ultrasonic agitation at 25 W for two hours. This step aids the homogenous incorporation of MWCNT in the PEO matrix. Samples with 5, 15, 25, 33, 40 and 50% wt. loadings of MWCNT were fabricated. Then the composites in liquid form were placed in Petri dishes and left for several days to dry in air at room temperature. Dried films were analyzed using Raman spectroscopy at 532 nm and scanning electron microscopy.

To fabricate the acetone sensors, dried composite films were cut into 1.5 cm x 1.0 cm pieces and silver paint electrodes were applied over about 0.3 mm at both edges. Acetone detection was achieved by measuring the changes in the sensor resistance due to acetone exposure using a computer controlled source meter unit. To achieve this, air at different flow rates was passed through a mixture of 25% acetone in water, to simulate different concentrations of acetone vapor exposure to the sensor. Typically, a constant voltage was applied across the PEO/MWCNT composite sensor and the change in resistance was derived from the change in the value of the measured current due to acetone exposure. Different concentration of acetone was simulated by varying the flow rate of air flowed through the 25% acetone in water solution to the sample surface. The relative response,  $A_r$  can be written as;

$$A_r = \frac{(R - R_o)}{R_o} \quad (1)$$

Where  $R_o$  and  $R$  are the resistance before and after exposure respectively. An average of five sensors on and off cycles was taken for each measurement.

### 3. Results

Fig. 1 shows the raman spectra for PEO/MWCNT composite acetone sensors before sensing (Fig. 1(a)) and after sensing (Fig. 1(b)). In (Fig. 1(a)) the uppermost plot obtained from pure MWCNT used in fabricating the composites and showed the typical spectrum for MWCNT. Three distinct peaks attributed to the D-line at about  $1338.8 \text{ cm}^{-1}$ , the G-line at  $1571.7 \text{ cm}^{-1}$  and the  $G'$ -line at  $2677.7 \text{ cm}^{-1}$  are clearly visible. The second trace in Fig. 1(a) shows the spectrum obtained from composite sample with 50% MWCNT loading. The D, G and  $G'$  peaks are present in addition to C-H stretching bands of PEO between  $2800 \text{ cm}^{-1}$  and  $3000 \text{ cm}^{-1}$  [24], their intensities are much lower than the  $G'$  band intensity. The third trace in Fig. 1(a) shows the spectrum of 40% MWCNT loading. It shows the same features as 50% with higher intensities in C-H stretching bands. The same can be said for samples with 33, 25, 15 and 5% wt. MWCNT loadings where the C-H bands have higher intensities compared to  $G'$  whenever the graphitic D, G and  $G'$  bands were more subdued. PEO has skeletal vibrations between  $400 \text{ cm}^{-1}$  and  $1500 \text{ cm}^{-1}$  as well as in the far infrared region at less than  $400 \text{ cm}^{-1}$  [24]. These bands were hardly visible for the sample with 50% wt. loading. However, in the samples with loadings lower than 50%, the PEO fingerprint and far infrared bands were evident. The ratios of their intensities to  $I_D$  and  $I_G$  bands depend inversely with CNT loading except for 15% sample.

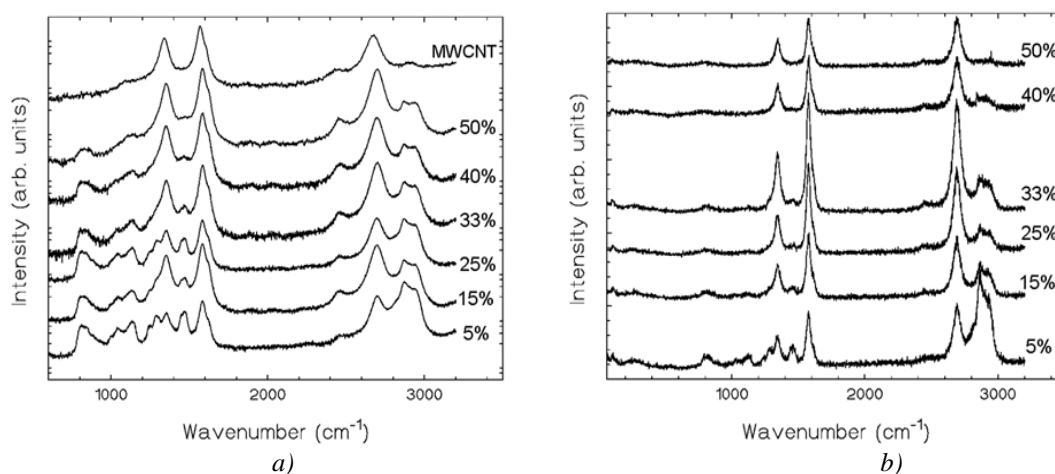
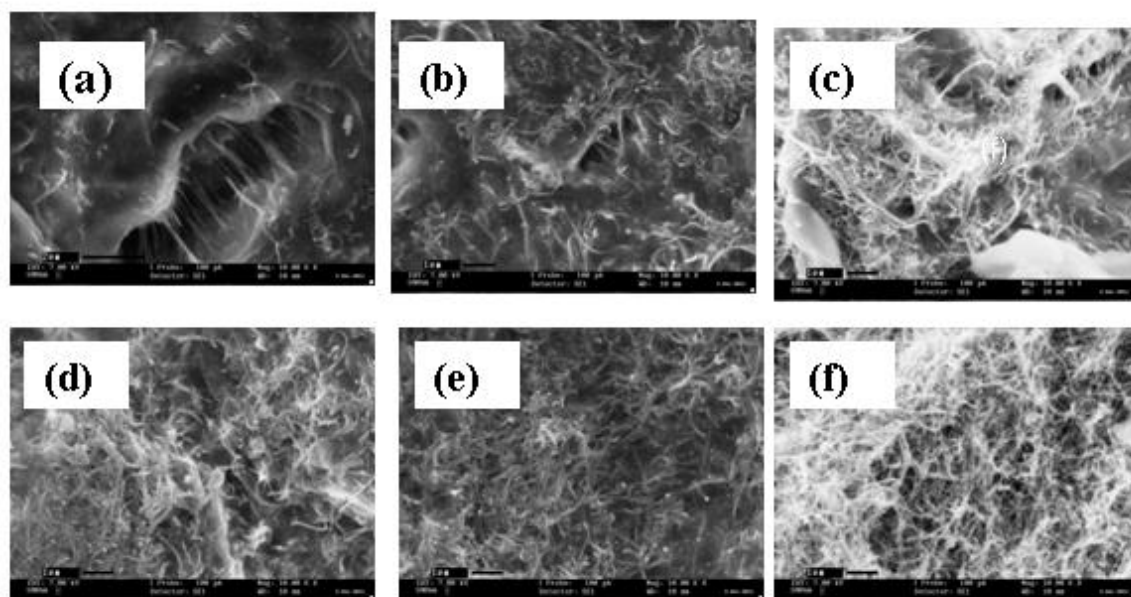


Fig.1. Raman spectroscopy of MWCNT/PEO films with different MWCNT loadings  
(a) Before sensing measurements. (b) After sensing measurements.

In order to evaluate the effect of acetone vapour on the composite, Raman measurements conducted on composite samples after exposure to acetone are shown in Fig. 1(b). Generally, the spectra were almost similar to that obtained before exposure except for a subtle difference where slight enhancement of the MWCNT peaks as compared to the PEO peaks was evident.

Fig. 2 (a) through to Fig. 2 (f) are SEM micrographs of composites with wt. % loadings of 5% through to 50%. The presence of MWCNT was evidently increasing with increasing MWCNT loading as expected.



*Fig. 2 SEM images of MWCNT/PEO films with (a) 5wt. %, (b) 15wt. %, (c) 25wt. %, (d) 33wt. %, (e) 40wt. % and (f) 50wt. %, MWCNT loadings.*

Fig. 3. Shows the time-dependent resistance response of the PEO/MWCNT composite acetone vapor sensors. Here, the changes in resistance in the sensor were measured upon 5 cycles. In each cycle, it was exposed for 3s to acetone vapour generated by bubbling air at flow rates of 10 to 100 sccm through a solution of 25% acetone in DI water, then left in the ambient air.

The results of the relative response and the sensitivity of the PEO/MWCNT film acetone sensors are summarized in Fig. 4. Fig. 4(a) shows the plots of the variation of PEO/MWCNT composite films relative response as a function of acetone concentration. The obvious trend observed was that the sensor sensitivity increased with decreasing MWCNT loadings in the composite sensor as evident by the gradient of the linear part of the curves in Fig.4(a). In addition, the variation of the sensor sensitivities with MWCNT loadings is shown in Fig. 4(b).

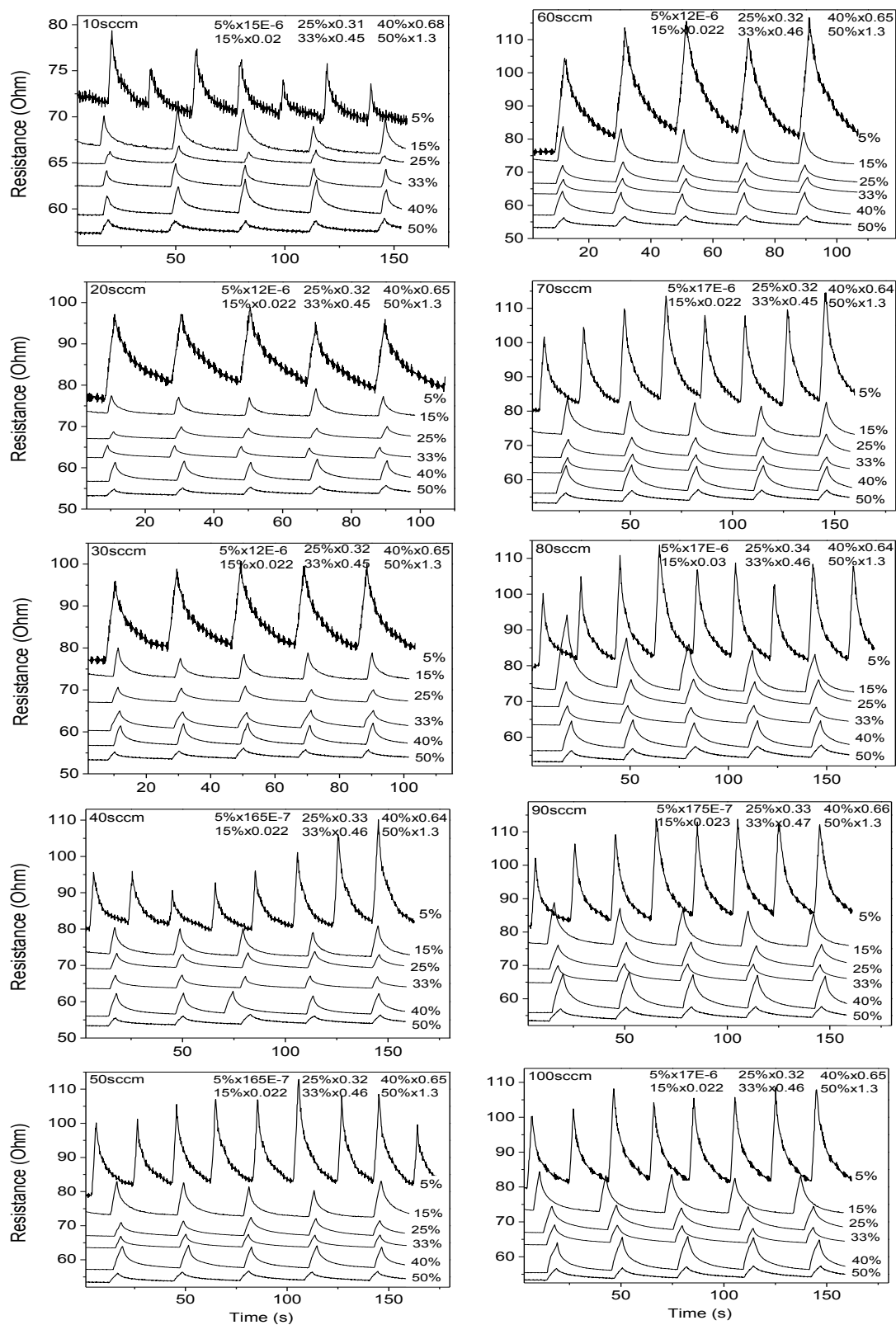


Fig.3. Five cycles of electrical response of PEO/MWCNT films with 5%, 15% and 25%, 33%, 40% and 50% wt. MWCNT loadings due to exposure to acetone vapor at flow rates from 10 to 100 sccm.

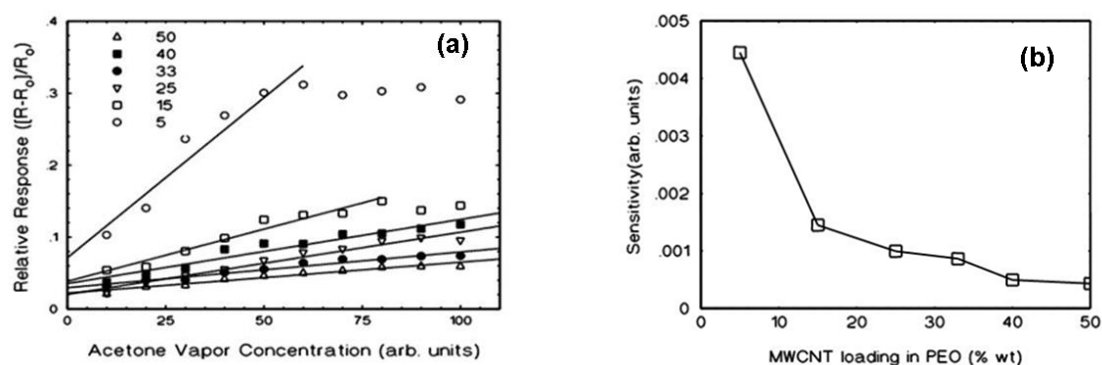


Fig. 4. (a) Variation of relative response with relative acetone concentration and (b) variation of sensitivity, of PEO/MWCNT films to acetone vapor at different MWCNT loadings.

#### 4. Discussion

In Fig. 1, the trend of diminishing Raman intensities of the PEO with increasing MWCNT loadings showed that MWCNT were well dispersed in the composites. After measurement, the slight enhancement of the MWCNT peaks as compared to the PEO can be due to the erosion of PEO surface from the composite due to acetone vapor exposure, resulting in surfaces with relatively enhanced MWCNT content when compared to before acetone vapor exposure. The SEM micrographs (Fig. 2) indicate the good distribution of MWCNT in the composites, which was supported by Raman spectroscopy results shown in Fig. 1 (a).

Regarding acetone sensing, the clear reproducible patterns suggest the vapour- sensor surface reaction while the gas is on and a fast recovery of a few seconds once it is off. The general trend of decreasing conductivity with decreasing MWCNT loadings is evident, with resistance increasing from  $42 \Omega$  for the sample with 50% wt. MWCNT content to almost  $10^7 \Omega$  for the sample with 5% wt. MWCNT (As mentioned in the graphs, some adjustments have been applied on resistance values). Concerning Fig. 4, saturation of measurements seemed to occur for sensor from films with the two lowest MWCNT loadings. Here, saturation occurred at 60 sccm for 5% wt. and at 70 sccm for 15% wt. MWCNT loading. The curves for samples with higher MWCNT loadings remained linear until 100 sccm and showed the trend of decreasing sensitivity with increasing MWCNT loadings. The observed phenomenon can be explained based on the mechanism of electrical conductivity in MWCNT. Basically, electrical conduction occurred through the motion of  $\pi$ - electrons on the MWCNT surfaces. At the lowest MWCNT loadings, composites conduct, albeit with high resistance and even though the MWCNT are not totally in contact with other spatially. Here, conduction also occur through a tunneling process where electrons may hop across two adjacent MWCNT situated at close distance. When used as acetone sensors, the response in terms of an increase in resistance was due to the adsorption of acetone molecules on the MWCNT surface. This resulted in the temporary immobilization of the  $\pi$ - electrons at the adsorption sites. As evident from the curves in Fig. 3, the sensors recovered their original resistance after less than 20 seconds. This may be due to desorption of the acetone molecules as result of local heating as a consequence of increased resistance. Table.1 shows the resistance and its rise and fall time in PEO/MWCNT composites under 50sccm flow rate.

Table 1. The resistance and its rise and fall time in PEO/MWCNT composites (50sccm).

CNT wt. %	Resistance ( $\Omega$ )	Rise time-Fall time (s)
5	$4 \times 10^6$	2.34-12.48
15	3332	1.82-7.02
25	209	2.08-10.4
33	138	1.82-9.36
40	87	2.08-8.58
50	41	2.6-14.29

The short rise and fall time indicate the easy reaction between the gas and the sensor surface. Based on this qualitative model, it is understandable that sensitivity increased and the dynamics decreased with decreasing MWCNT loading. The MWCNT loadings that a well dispersed PEO/MWCNT composited determined the surface area of MWCNT available and thus the number of  $\pi$ - electron sites. The high sensitivity was due to the high ratio of acetone molecules adsorbed to the number of sites available, thus elevating the values of relative response. At some point, a saturation was reached where no increase of resistance occurred. Where the acetone molecules overcame the sensing sites.

## 5. Conclusions

The effects of MWCNT loading in PEO/MWCNT composite sensor on its sensitivity and dynamic range to acetone vapour exposure have been studied. In general, PEO/MWCNT composites have been shown to be an efficient sensor for acetone sensor, where the composite material can be easily incorporated in actual devices. We have discovered that the sensitivity increased with decreasing MWCNT loadings while the dynamic range generally decreased with decreasing MWCNT loadings. We have demonstrated that there is a tradeoff between sensitivity and dynamic range as a result of MWCNT loadings. Highest sensitivities were afforded at low MWCNT loadings of 5 and 15% wt. showed saturation of measurements. At higher MWCNT loadings no saturation of measurements were observed for the range of measurement conducted. The phenomenon was explained in terms of the electrical conductivity mechanism in MWCNT, which involved  $\pi$ - electrons and the sensor response in terms of increase in resistance were due to immobilization of  $\pi$ - electron as a result of acetone molecules adsorbed on  $\pi$ - electron sites.

## Acknowledgements

This work is funded by the Ministry of Higher Education of Malaysia under the FRGS grant No. FP008/2010C.

## References

- [1] G. J.Sun, H.Kheel, S. Park, S. Lee, S. E. Park, &C. Lee, *Ceramics International* **42**(1), 1063(2016).
- [2] T.Hu, X. Chu, F.Gao, Y.Dong, W. Sun, &L. Bai, *Materials Science in Semiconductor Processing* **34**, 146 (2015).
- [3] A.D. Wilson, M. Baietto, *Sensors* **11**, 1105 (2011).
- [4] S.Salehi, E. Nikan, A. A.Khodadadi, &Y. Mortazavi, *Sensors and Actuators B: Chemical* **205**, 261(2014).
- [5] C. Deng, J. Zhang, X. Yu, W. Zhang, X. Zhang, *Journal of chromatography. B, Analytical technologies in the biomedical and life sciences* **810**, 269 (2004)
- [6] T. Mottram, P. Dobbelaar, Y. Schukken, P. Hobbs, P. Bartlett, *Livestock production science*

- 61**, 7 (1999).
- [7] N. Rezlescu, N. Iftimie, E. Rezlescu, C. Doroftei, P. Popa, *Sensors and Actuators B: Chemical* **114**, 427 (2006).
- [8] H. Lord, Y. Yu, A. Segal, J. Pawliszyn, *Analytical chemistry* **74**, 5650 (2002).
- [9] C. Wang, A. Mbi, *Measurement Science and Technology* **18**, 2731 (2007).
- [10] C. Wang, P. Sahay, *Sensors* **9**, 8230 (2009).
- [11] W. Ping, T. Yi, X. Haibao, S. Farong, *Biosensors and bioelectronics* **12**, 1031 (1997).
- [12] M. Suresh, N. J.Vasa, V.Agarwal, &J. Chandapillai, presented at the 36th Annual International Conference In Engineering in Medicine and Biology Society (2014, August), IEEE (pp. 3476-3479) 2014.
- [13] K. Awasthi, S. Awasthi, A. Srivastava, R. Kamalakaran, S. Talapatra, P. Ajayan, O. Srivastava, *Nanotechnology* **17**, 5417 (2006).
- [14] M. Park, H. Kim, J.P. Youngblood, S.W. Han, E. Verploegen, A.J. Hart, *Nanotechnology* **22**, 415703 (2011).
- [15] M.T. Müller, B. Krause, P. Pötschke, *Polymer* **53**(15), 3083 (2012).
- [16] J. Lu, B. Kumar, M. Castro, J.F. Feller, *Sensors and Actuators B: Chemical* **140**, 451 (2009)
- [17] Q. Fan, Z. Qin, T. Villmow, J. Pionteck, P. Pötschke, Y. Wu, B. Voit, M. Zhu, *Sensors and Actuators B: Chemical* **156**, 63 (2011).
- [18] B.Bhowmik, K.Dutta, A. Hazra, &P. Bhattacharyya, *Solid-State Electronics* **99**, 84 (2014).
- [19] D.An, X.Tong, J.Liu, Q. Wang, Q. Zhou, J.Dong, &Y. Li, *Superlattices and Microstructures* **77**, 1 (2015).
- [20] A.Rydosz, A. Szkudlarek, M.Ziabka, K. Domanski, W.Maziarz, &T. Pisarkiewicz, *IEEE Sensors Journal* **16**, 1004 (2016).
- [21] A. Bouvree, J. F.Feller, M.Castro, Y. Grohens, &, M. Rinaudo, *Sensors and Actuators B: Chemical*, **138**, 138(2009).
- [22] Q. Fan, Z. Qin, T. Villmow, J. Pionteck, P.Pötschke, Y.Wu, &M. Zhu, *Sensors and Actuators B: Chemical* **156**, 63 (2011).
- [23] B.Kumar, M.Castro, &J. F. Feller, *Chem. Sens*, **3**, 1(2013).
- [24] Q. Zhang PhD Thesis University of Chalmers, Goteborg, Sweden (2011).